

## Intrauterine growth-restricted sheep fetuses exhibit smaller hindlimb muscle fibers and lower proportions of insulin-sensitive Type I fibers near term

Dustin T. Yates,<sup>1,2</sup> Caitlin N. Cadaret,<sup>1</sup> Kristin A. Beede,<sup>1</sup> Hannah E. Riley,<sup>1</sup> Antoni R. Macko,<sup>2</sup> Miranda J. Anderson,<sup>2</sup> Leticia E. Camacho,<sup>2</sup> and Sean W. Limesand<sup>2</sup>

<sup>1</sup>Department of Animal Science, University of Nebraska, Lincoln, Nebraska; and <sup>2</sup>School of Animal and Comparative Biomedical Sciences, The University of Arizona, Tucson, Arizona

Submitted 16 December 2015; accepted in final form 29 March 2016

**Yates DT, Cadaret CN, Beede KA, Riley HE, Macko AR, Anderson MJ, Camacho LE, Limesand SW.** Intrauterine growth-restricted sheep fetuses exhibit smaller hindlimb muscle fibers and lower proportions of insulin-sensitive Type I fibers near term. *Am J Physiol Regul Integr Comp Physiol* 310: R1020–R1029, 2016. First published April 6, 2016; doi:10.1152/ajpregu.00528.2015.—Intrauterine growth restriction (IUGR) reduces muscle mass and insulin sensitivity in offspring. Insulin sensitivity varies among muscle fiber types, with Type I fibers being most sensitive. Differences in fiber-type ratios are associated with insulin resistance in adults, and thus we hypothesized that near-term IUGR sheep fetuses exhibit reduced size and proportions of Type I fibers. Placental insufficiency-induced IUGR fetuses were ~54% smaller ( $P < 0.05$ ) than controls and exhibited hypoxemia and hypoglycemia, which contributed to 6.9-fold greater ( $P < 0.05$ ) plasma norepinephrine and ~53% lower ( $P < 0.05$ ) plasma insulin concentrations. IUGR semitendinosus muscles contained less ( $P < 0.05$ ) myosin heavy chain-I protein (MyHC-I) and proportionally fewer ( $P < 0.05$ ) Type I and Type I/IIa fibers than controls, but MyHC-II protein concentrations, Type II fibers, and Type IIx fibers were not different. IUGR biceps femoris muscles exhibited similar albeit less dramatic differences in fiber type proportions. Type I and IIa fibers are more responsive to adrenergic and insulin regulation than Type IIx and may be more profoundly impaired by the high catecholamines and low insulin in our IUGR fetuses, leading to their proportional reduction. In both muscles, fibers of each type were uniformly smaller ( $P < 0.05$ ) in IUGR fetuses than controls, which indicates that fiber hypertrophy is not dependent on type but rather on other factors such as myoblast differentiation or protein synthesis. Together, our findings show that IUGR fetal muscles develop smaller fibers and have proportionally fewer Type I fibers, which is indicative of developmental adaptations that may help explain the link between IUGR and adulthood insulin resistance.

fetal growth restriction; fetal programming; myocyte

A GROWING NUMBER OF STUDIES have linked intrauterine growth restriction (IUGR) to insulin resistance, obesity, and metabolic syndrome later in life (5, 31, 59, 61, 62, 68, 81). The fetal adaptations underlying these complications have not been fully characterized but likely include structural and functional changes in skeletal muscle development, since muscle is the primary site for insulin-stimulated glucose disposal (27). Throughout life, IUGR-born individuals generally exhibit less muscle mass and greater central fat deposition (3, 33, 43, 90), and we recently showed that semitendinosus muscle fibers in IUGR fetal sheep are smaller near term due in part to impaired myoblast proliferative capacity (86). Moreover, protein analysis of muscle samples in other

studies have shown evidence of impaired insulin signaling (39, 40, 63, 64). Reduced muscle growth and insulin-stimulated glucose consumption may represent essential nutrient-sparing adaptations in IUGR fetuses but also likely contribute to insulin resistance and metabolic dysfunction in adulthood (87, 89).

Skeletal muscle is composed of heterogeneous populations of muscle fibers that can be classified by expression of different myosin heavy chain (MyHC) isoforms, and rat studies have shown that responsiveness to insulin differs among fiber types (34, 38, 55). Insulin-stimulated glucose uptake rates are greatest in Type I fibers (slow oxidative; MyHC-I) and lowest in Type IIx fibers (fast glycolytic; MyHC-IIx). The response of Type IIa fibers (fast oxidative/glycolytic; MyHC-IIa) to insulin is intermediate between Type I and Type IIx myofibers. Each skeletal muscle is composed of specific fiber-type ratios, and composition differences in thigh muscles have been associated with insulin resistance in adult men (40, 49). We postulate that IUGR conditions alter fetal fiber-type ratios in a way that promotes development of insulin resistance in IUGR skeletal muscle. Specifically, we would expect reduced proportions of the most insulin-sensitive fiber type: Type I fibers. Furthermore, reductions in size may occur disproportionately in Type I fibers and result in further decreases in insulin sensitivity.

The objective of this study was to determine whether fiber type-specific differences in size and ratios occur in IUGR fetal skeletal muscles near the end of gestation. The study was performed using a well-characterized IUGR model (26, 54, 71, 72) in which pregnant ewes are exposed to high ambient temperatures for an extended period during midgestation to generate natural placental insufficiency (11, 14, 32, 71). In these animals, the reduced size and transport capacity (11, 69, 70, 80) of the placenta prevent it from meeting the nutrient requirements for rapid fetal growth that occurs late in gestation, after animals are returned to thermoneutral conditions. Hyperthermia-induced placental insufficiency results in patterns of progressively worsening hypoxemia, hypoglycemia, and asymmetrical fetal growth restriction (22, 48, 51, 53) congruent to other models of placental insufficiency (21, 23–25, 46, 60, 84) as well as humans (30, 36, 76). We evaluated two commonly studied mixed-fiber type hindlimb muscles, the semitendinosus and biceps femoris, that are similar-sized and adjacently located. Under normal circumstances these muscles express comparable fiber sizes, fiber-type ratios, and metabolic enzyme profiles (35, 42, 44) but differences in vascularity and innervation (67, 85), as well as temporal aspects of development (29).

Address for reprint requests and other correspondence: D. Yates, PO Box 830908, Lincoln, NE 68583 (e-mail: dustin.yates@unl.edu).

## MATERIALS AND METHODS

**Animals and experimental treatments.** Animal care and use was approved by the Institutional Animal Care and Use Committee at The University of Arizona, Tucson, AZ, which is accredited by the American Association for Accreditation of Laboratory Animal Care. Animal studies were performed at the University of Arizona Agricultural Research Complex.

Columbia-Rambouillet crossbred ewes with singleton pregnancies confirmed by ultrasound were obtained from Nebeker Ranch (Lancaster, CA). IUGR fetuses ( $n = 7$ ; 4 male, 3 female) were generated by inducing placental insufficiency as previously described (48, 53). Briefly, pregnant ewes were exposed to elevated ambient temperatures (40°C for 12 h/day, 35°C for 12 h/day; dew point 22°C) from the 40th to the 95th day of gestational age (dGA). Age-matched control fetuses ( $n = 6$ ; 3 male, 3 female) were generated from ewes housed at 25°C and pair-fed to the average daily intake of the IUGR group. At 120 ± 1 dGA, indwelling polyvinyl catheters were surgically placed in the fetal abdominal aorta via the hindlimb pedal artery as previously described (50, 52). Catheters were tunneled subcutaneously to the flank of the ewe and exteriorized. At 132 ± 1 dGA, a series of three fetal blood samples were collected from each animal in 5-min intervals as previously described (48, 88). Ewes and fetuses were euthanized at 134 ± 1 dGA with Euthasol (Merck Animal Health). Fetal, placental, and organ weights were measured postmortem. Fetal semitendinosus and biceps femoris muscles were collected for immunohistochemistry and gene expression analysis.

**Blood sample analysis.** Fetal blood samples were analyzed as previously described (48, 88). Whole blood oxygen, carbon dioxide, and pH levels were determined with an ABL 720 blood gas analyzer (Radiometer, Copenhagen, Denmark). Plasma glucose and lactate concentrations were determined with an YSI 2700 SELECT biochemistry analyzer (Yellow Springs Instruments, Yellow Springs, OH). Plasma insulin and norepinephrine concentrations were determined by commercial ELISA kits (Ovine Insulin, ALPCO Diagnostics, Windham, NH; 2-CAT, Rocky Mountain Diagnostics, Colorado Springs, CO) as previously described (88), with intra-assay and inter-assay coefficients of variance of less than 15% for each.

**Immunohistochemistry.** Central, cross-sectional biopsies of the semitendinosus and biceps femoris muscles were fixed in 4% paraformaldehyde and phosphate-buffered saline (PBS; pH 7.3), embedded in OTC Compound, and frozen as previously described (18, 86). Eight-micrometer sections were mounted on Fisherbrand Superfrost Plus microscope slides (Thermo Fisher Scientific, Waltham, MA) and immunostained. Briefly, tissues were washed in PBS with 0.1% Triton-X-100 (Sigma-Aldrich) and then steamed with 10 mM citric acid buffer (pH 6; Sigma-Aldrich) for antigen retrieval. Nonspecific binding was blocked with 0.5% NEN blocking buffer (Perkin-Elmer, Waltham, MA). Primary antiserum diluted in PBS + 1% bovine serum albumin was applied overnight at 4°C (primary antiserum was excluded in negative controls). Fiber types were determined with antibodies raised in the mouse against MyHC-I (BA-D5, 1:20; DSHB, University of Iowa, Iowa City, IA), MyHC-II (F18, 1:20; DSHB),

Table 2. Morphometric data

Variable	Control ( $n = 6$ )	IUGR ( $n = 7$ )	<i>P</i> Value
dGA	135 ± 0.5	134 ± 0.5	NS
Uteroplacental mass, g			
Uterus	491 ± 48	398 ± 48	NS
Placenta	297 ± 31	131 ± 29	<0.01
Number of placentomes	89.3 ± 6.6	74.2 ± 6.2	NS
Average placentome mass, g	3.34 ± 0.33	2.01 ± 0.31	<0.01
Fetal mass, g			
Fetus	3,279 ± 199	1,491 ± 184	<0.01
Carcass	2,531 ± 152	1,098 ± 141	<0.01
Carcass/fetus, %	77.2 ± 0.6	73.5 ± 0.6	<0.01
Relative organ mass, g/fetal kg			
Brain	16.2 ± 2.6	29.9 ± 2.4	<0.01
Heart	6.9 ± 0.3	8.5 ± 0.2	<0.01
Liver	26.5 ± 2.3	30.1 ± 2.2	NS
Lungs	28.3 ± 1.5	32.0 ± 1.4	NS
Kidneys	6.5 ± 0.9	8.3 ± 0.9	NS
Spleen	2.9 ± 0.3	2.0 ± 0.3	NS

Values are means ± SE; *n*, number of animals. NS, not significant.

MyHC-I/MyHC-IIa (BF-32, 1:20; DSHB), and MyHC-IIx (6H1, 1:150; DSHB) (13). Fibers were counterstained with rabbit antidesmin (1:200; Sigma-Aldrich). Immunocomplexes were detected with affinity-purified immunoglobulin antiserum conjugated to Alexa Fluor 594 (1:3,000; Invitrogen Life Technologies, Carlsbad, CA) or Alexa Fluor 488 (1:2,500; Jackson ImmunoResearch Laboratories, West Grove, PA). Fluorescent images were visualized on a Leica DM5500 microscope system and digitally captured with a Spot Pursuit 4 Megapixel CCD camera (Diagnostic Instruments, Sterling Heights, MI). Images were analyzed with Image Pro Plus 6.3 software (Media Cybernetics, Silver Spring, MD) and ImageJ (National Institutes of Health, Bethesda, MD) to determine fiber-type proportions and mean cross-sectional areas. To prevent evaluator bias during morphometric assessment, histological images were encoded to conceal animal and treatment designations.

**Myosin heavy chain electrophoresis.** Snap-frozen muscle samples (50 mg) were homogenized in 200 µl of RIPA buffer containing manufacturer recommended concentrations of Halt Protease and Halt Phosphatase Inhibitor Cocktails (Thermo Fisher). Homogenates were then sonicated and centrifuged (2500 g; 10 min), and supernatant was collected. Total protein concentrations were determined by Pierce BCA Assay (Thermo Fisher). Samples were incubated at room temperature for 10 min, heated at 70°C for 10 min, combined with Bio-Rad 4× Laemmli Sample Buffer (Bio-Rad, Hercules, CA) to a 1× concentration, and loaded at 10 µg/well. MyHC isoforms were separated by SDS-PAGE (66, 78). Stacking gels consisted of 47% vol/vol glycerol (100%), 6% vol/vol acrylamide-bisacrylamide (50:1), 110 mM Tris (pH 6.7), 6 mM EDTA, 0.4% vol/vol SDS (10%), 0.1% vol/vol ammonium persulfate (10%), and 0.05% vol/vol tetramethyl-

Table 1. Primers for qPCR

Gene	Protein	Primer Sequence	Product Size	Accession Number
<i>MYH7</i>	MyHC-I	GAG ATG GCC GCG TTT GGG GAG GGC TCG TGC AGG AAG GTC AGC	283	AB058898.1
<i>MYH2</i>	MyHC-IIa	ACC GAA GGA GGG GCG ACT CTG GGC TCG TGC AGG TGG GTC ATC	109	AB058896.1
<i>MYH1</i>	MyHC-IIx	AAA GCG ACC GTG CAG AGC AGG GGC TCG TGC AGG TGG GTC ATC	154	AB058897.1
<i>RPS15</i>	s15	ATC ATT CTG CCC GAG ATG GTG TGC TTT ACG GGC TTG TAG GTG	134	AY949774.1

MYH, myosin heavy chain.

Table 3. Fetal blood and plasma parameters

Variable	Control (n = 6)	IUGR (n = 7)	P Value
Plasma norepinephrine, pg/ml	323 ± 303	2216 ± 208	<0.01
Plasma insulin, ng/ml	0.32 ± 0.05	0.15 ± 0.05	0.04
Plasma glucose, mM	1.05 ± 0.10	0.69 ± 0.09	0.02
Plasma lactate, mM	1.82 ± 0.33	3.02 ± 0.31	0.02
Blood O <sub>2</sub> , mM	3.40 ± 0.23	2.15 ± 0.21	<0.01
Blood O <sub>2</sub> saturation, %	48.0 ± 5.2	31.7 ± 4.8	0.04

Values are means ± SE; n, number of animals. IUGR, intrauterine growth restriction.

ethylenediamine (TEMED, 100%). Resolving gels were composed of 35% vol/vol glycerol (100%), 9% vol/vol acrylamide-bisacrylamide (50:1), 230 mM Tris (pH 8.8), 115 mM glycine, 0.4% vol/vol SDS (10%), 0.1% vol/vol ammonium per sulfate (10%), and 0.05% vol/vol TEMED (100%). The upper running buffer consisted of 100 mM Tris, 150 mM glycine, 0.1% SDS, and 0.07% 2β-mercaptoethanol in distilled water, and the lower running buffer consisted of 50 mM Tris, 75 mM glycine, and 0.05% SDS in distilled water. Electrophoresis was performed on a Mini-PROTEAN Tetra Cell (Bio-Rad) at 4°C for 24 h at a constant 150 V. After electrophoresis, gels were stained overnight with Gel-Code Blue (Thermo Fisher), destained in distilled water, and imaged on an Odyssey infrared imaging system (LI-COR Biosciences, Lincoln, NE). MyHC-I and collective MyHC-II bands were measured by densitometry (Image Studio Lite Ver 5.0; LI-COR).

**Myosin heavy chain Western immunoblot.** Skeletal muscle proteins were separated by SDS-PAGE and transferred to polyvinylidene fluoride membranes as previously described (17, 52). Membranes were incubated in Tris-buffered saline + 0.1% Tween-20 + 5% nonfat dry milk for 1 h to block nonspecific binding and then incubated overnight at 4°C with mouse anti-MyHC-I or MyHC-II primary antibodies diluted in Tris-buffered saline + 0.1% Tween-20 + 5% nonfat dry milk. MyHC immunoblots were normalized to β-tubulin (1:3,000; RB-9249, Thermo Fisher). Immunocomplexes were detected with goat antimouse IgM horseradish peroxidase-conjugated secondary antibody (1:5,000; Santa Cruz Biotechnology, Santa Cruz, CA) or with goat antimouse IgG horseradish peroxidase-conjugated secondary antibody (1:20,000; Bio-Rad) using West Pico Chemiluminescent Substrate (Thermo Scientific, Rockford, IL) and exposed to X-ray film. Densitometry values were determined with ImageJ software.

**Quantitative PCR.** RNA was extracted from ground muscle (200 mg) using the QIAprep Spin MiniPrep kit (Qiagen, Valencia, CA) and was reverse transcribed in triplicate (16). Oligonucleotide primers (Table 1) were synthesized as previously described (17) and PCR products were cloned into pCR II (Invitrogen) and confirmed with nucleotide sequencing (University of AZ Genetics Core, Tucson, AZ) (16). Primer efficiencies and standard curves were determined from plasmid DNA, which were linear over six orders of magnitude. Concentrations of mRNA for each gene were determined by qPCR using SYBR Green (Qiagen) in an iQ5 Real-Time PCR Detection System (Bio-Rad Laboratories). Samples were initially denatured (95°C for 15 min) and then amplified with 45 cycles of denaturing (96°C for 30 s), annealing (60–62°C for 30 s), and fluorescence measurement during extension (72°C for 10 s). Melt curves were performed after amplification to confirm product homogeneity. mRNA concentrations for each gene of interest were determined from triplicate cDNA and normalized to mRNA concentrations of ribosomal protein s15.

**Statistical analysis.** All data were analyzed by ANOVA using the GLM procedure of SAS (SAS Institute, Cary NC) to determine treatment effects. Fetal sex was initially included as a covariate in all analysis but was only significant for liver weight and was removed from the model for all other parameters. For each fetus, values for

whole blood and plasma parameters represent the average of the three blood samples. Mean semitendinosus and biceps femoris muscle fiber cross-sectional areas were determined from a minimum of 300 fibers across 10 nonoverlapping fields of view. The percentages of fibers staining positive for each MyHC were determined from a minimum of 1,500 fibers per muscle. MyHC mRNA concentrations normalized to the s15 housekeeping gene are expressed as the amount relative to controls. Individual MyHC protein concentrations analyzed by electrophoresis are expressed as the percentage of total MyHC protein. Individual MyHC protein concentrations analyzed by Western immunoblot were normalized to β-tubulin protein content and are expressed as the relative density compared with controls. Pearson correlation analyses were performed using the CORR procedure of SAS. All data are expressed as means ± SE.

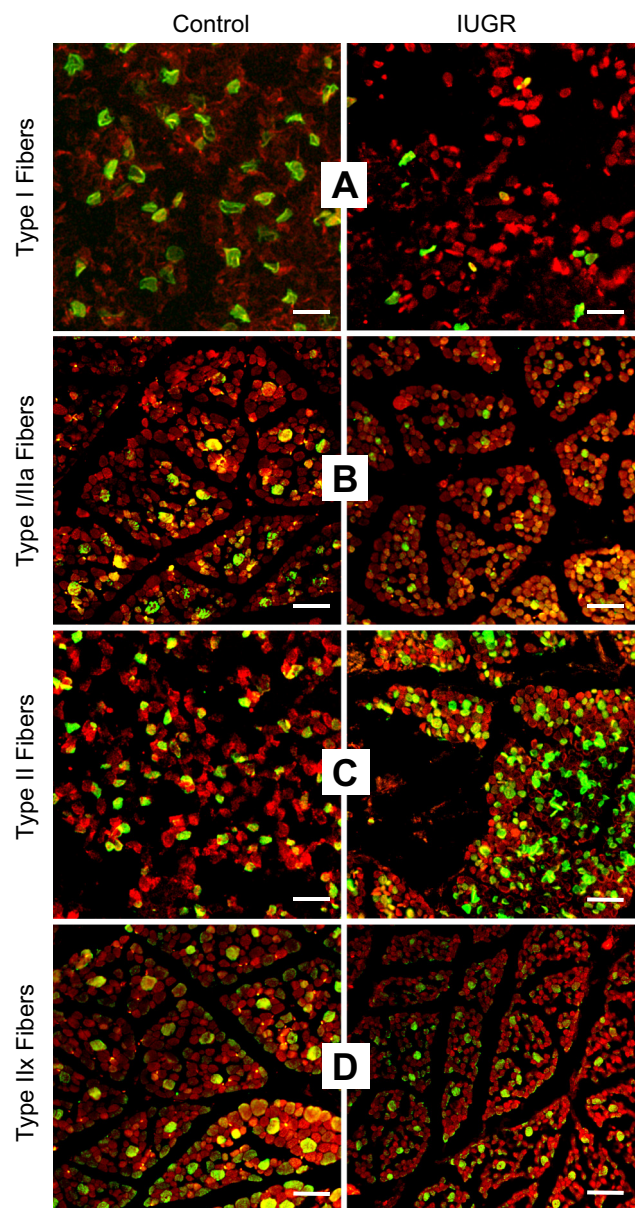
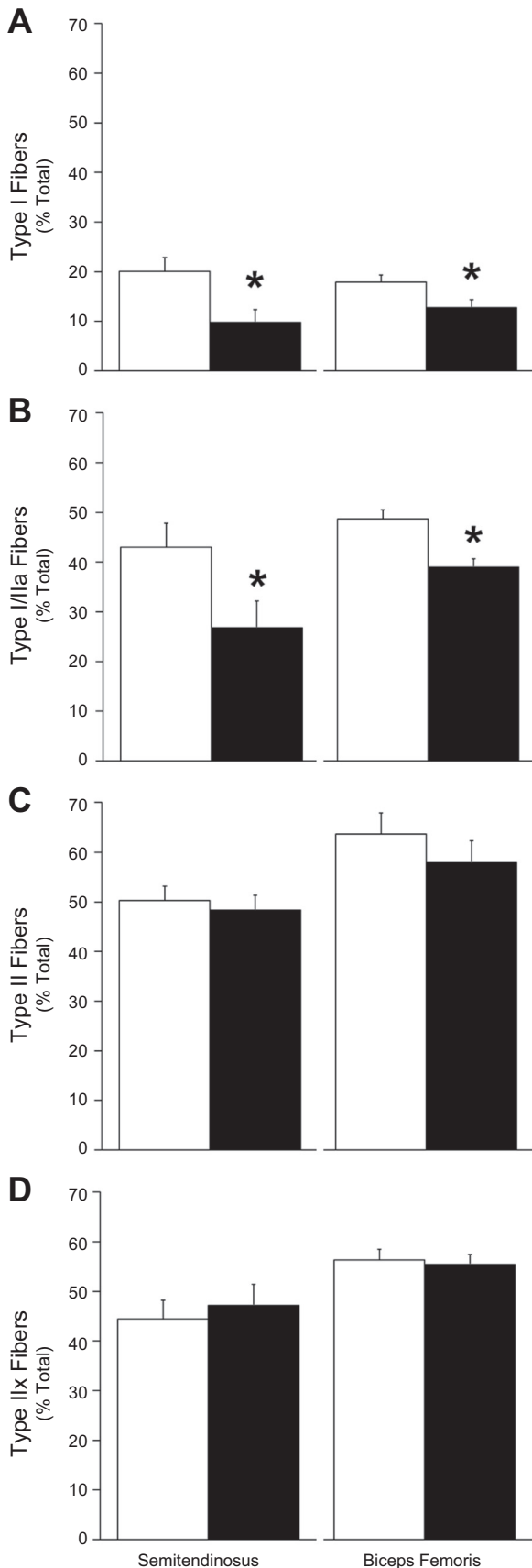


Fig. 1. Immunostaining for fiber type in fetal semitendinosus muscles. Representative micrographs are depicted for control and intrauterine growth restriction (IUGR) semitendinosus cross sections (8 μm). Sections were stained for myosin heavy chain (MyHC) isoforms (green) and counterstained for desmin (red). A: Type I fibers (MyHC-I); B: Types I or IIa fibers (MyHC-I/IIa); C: Type II fibers (MyHC-II); D: Type IIx fibers (MyHC-IIx). White magnification bar = 50 μm.



## RESULTS

**Morphometrics.** Uterine weights were not different between ewes carrying IUGR and control fetuses (Table 2), but placentas from IUGR fetuses weighed  $\sim 65\%$  less ( $P < 0.05$ ) than placentas from controls. The number of placentomes was not different between IUGR and control fetuses, but average weight per placentome was less ( $P < 0.05$ ) in IUGR fetuses.

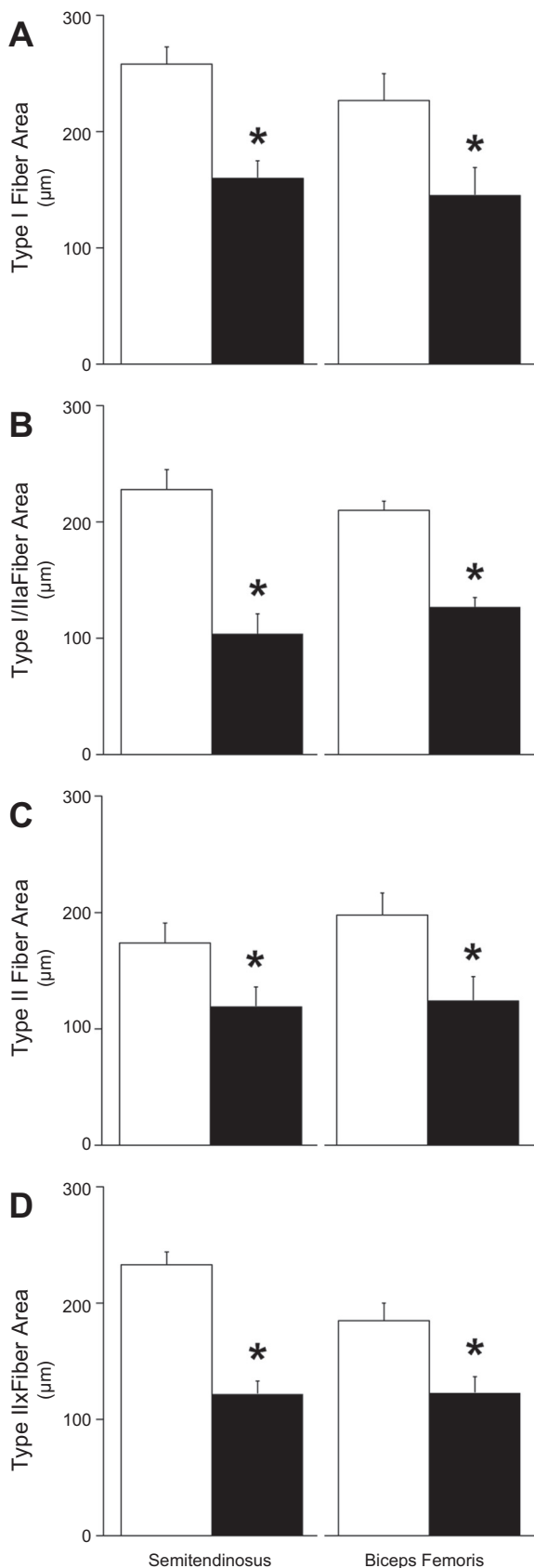
IUGR fetuses were  $\sim 65\%$  lighter than controls ( $P < 0.05$ ; Table 2). Carcass weight and carcass weight/fetal weight were also lower ( $P < 0.05$ ) in IUGR fetuses. When compared with controls, IUGR fetal brain, heart, lungs, kidneys, and spleen were smaller ( $P < 0.05$ ; data not shown). Liver was also smaller ( $P < 0.05$ ) in females than males, but fetal sex and fetal treatment group did not interact. When normalized to fetal weight (Table 2), relative brain and heart weights were greater ( $P < 0.05$ ) in IUGR fetuses and relative liver, lung, kidney, and spleen weights were not different compared with controls.

**Fetal blood and plasma analysis.** Plasma norepinephrine concentrations were  $\sim 690\%$  greater ( $P < 0.05$ ) and plasma insulin concentrations were  $\sim 53\%$  less ( $P < 0.05$ ) in IUGR fetuses than in controls (Table 3). IUGR fetuses also had lower ( $P < 0.05$ ) plasma glucose concentrations and higher ( $P < 0.05$ ) plasma lactate concentrations than controls. Blood oxygen content and saturation were both lower ( $P < 0.05$ ) in IUGR fetuses compared with controls. Partial pressure of carbon dioxide was not different between the two groups.

**Fiber type distribution and size.** Proportions of Type I fibers, Type II fibers, combined Type I/IIa fibers, and Type IIx fibers were identified by MyHC staining (Fig. 1). The proportion of Type I fibers and the combined proportion of Type I/IIa fibers were less ( $P < 0.05$ ) in IUGR fetuses than in controls for both semitendinosus and biceps femoris muscles (Fig. 2), but the proportion of Type II fibers and the proportion of Type IIx fibers were not different between IUGR and control fetuses for either muscle. Average cross-sectional areas were lower ( $P < 0.05$ ) for all fiber types in IUGR muscles compared with controls (Fig. 3). Proportions of Type I/IIa fibers in semitendinosus muscle and Type II fibers in biceps femoris muscles were positively correlated ( $P < 0.05$ ) with plasma insulin concentrations ( $r = 0.62$  and  $0.65$ , respectively). Proportions of Type I and Type I/IIa fibers in semitendinosus muscles ( $r = -0.64$  and  $-0.68$ , respectively) and biceps femoris muscles ( $r = -0.45$  and  $-0.70$ , respectively) were negatively correlated ( $P < 0.05$ ) with plasma norepinephrine concentrations.

**Skeletal muscle protein.** The percentage of total MyHC that was identified by protein electrophoretic mobility as MyHC-I was lower ( $P < 0.05$ ) and the percentage identified as MyHC-II was greater ( $P < 0.05$ ) in IUGR than in control semitendinosus muscles (Fig. 4A). However, no differences in MyHC-I or MyHC-II percentages of total MyHC were observed between IUGR and control biceps femoris muscles.

Fig. 2. Muscle fiber-type proportions. The percentages of total fibers (means  $\pm$  SE) are presented for control and IUGR fetal semitendinosus and biceps femoris muscle sections. Control, open bars; IUGR, black bars. A: Type I fibers (MyHC-I positive); B: Types I or IIa fibers (MyHC-I/IIa positive); C: Type II fibers (MyHC-II positive); D: Type IIx fibers (MyHC-IIx positive) were determined by immunostaining. All sections were counterstained for desmin to determine total fiber numbers. \*Differences ( $P < 0.05$ ) between control and IUGR groups within each muscle.



Immunoblot analysis showed less ( $P < 0.05$ ) MyHC-I in IUGR semitendinosus muscles than in controls but similar concentrations of MyHC-II between the two groups (Fig. 4B).

**Myosin heavy chain gene expression.** MyHC-I mRNA concentrations were less ( $P < 0.05$ ) in IUGR semitendinosus muscle but greater ( $P < 0.05$ ) in IUGR biceps femoris muscle compared with controls (Fig. 5). IUGR fetuses contained less ( $P < 0.05$ ) MyHC-IIa mRNA than controls in both semitendinosus and biceps femoris muscles. MyHC-IIx mRNA concentrations were not different between the two groups in either muscle.

#### DISCUSSION

Our findings in hindlimb muscles from near-term fetal sheep show that placental insufficiency-induced IUGR reduces the proportion of Type I fibers alone as well as the collective proportion of Types I and IIa, but does not alter the total proportion of Type II fibers or the proportion of the Type IIx subgroup. Size, however, was reduced in all IUGR fibers regardless of type. Skeletal muscle is the principal tissue for insulin-stimulated glucose utilization, and muscle mass and fiber type composition greatly affect insulin sensitivity and glucose homeostasis (34, 38, 55). Thus smaller fibers and less Type I and IIa fibers may begin to explain the link between IUGR and skeletal muscle insulin resistance in adulthood (40, 63). Our morphometric data show that the fetal response to placental insufficiency included asymmetric growth restriction in which fetal carcass weight was diminished to a greater extent than fetal body weight. Disproportional reduction of lean tissue, especially muscle, is a hallmark of IUGR fetuses (12, 47, 65) that has been shown to continue throughout the lifespan of the offspring (3, 33, 43, 82, 90), leaving them at greater risk for metabolic disorders (5, 28, 61, 68, 81). Decreased oxygen and nutrient supply to the fetus due to placental insufficiency make nutrient-sparing adaptations necessary for survival, and the high metabolic plasticity of skeletal muscle makes it an ideal tissue for nutrient sparing, even at the expense of growth (87, 89). Indeed, our findings indicate that fetal adaptations to IUGR conditions alter fiber-type ratios and restrict hypertrophy of all fibers in two postural hindlimb muscles, which would be consistent with less capacity for insulin-stimulated glucose utilization.

The proportions of Type I fibers alone and the combined proportions of Types I and IIa fibers in semitendinosus and biceps femoris muscles were substantially reduced by IUGR, but proportions of total Type II fibers and of Type IIx fibers were not affected. We attribute these changes in fiber composition to differences in the responsiveness of each fiber type to the conditions caused by placental insufficiency. Our IUGR fetuses suffered from a ~40% reduction in blood oxygen content that stimulated a near sevenfold increase in circulating norepinephrine, the main catecholamine secreted by the pre-

Fig. 3. Muscle fiber cross-sectional areas. Fiber cross-sectional areas (means  $\pm$  SE) are presented for control and IUGR fetal semitendinosus and biceps femoris muscle sections. Control, open bars; IUGR, black bars. A: Type I fibers (MyHC-I positive); B: Types I or IIa fibers (MyHC-I/IIa positive); C: Type II fibers (MyHC-II positive); D: Type IIx fibers (MyHC-IIx positive) were determined by immunostaining. All sections were counterstained for desmin to determine total fiber numbers. \*Differences ( $P < 0.05$ ) between control and IUGR groups within each muscle.

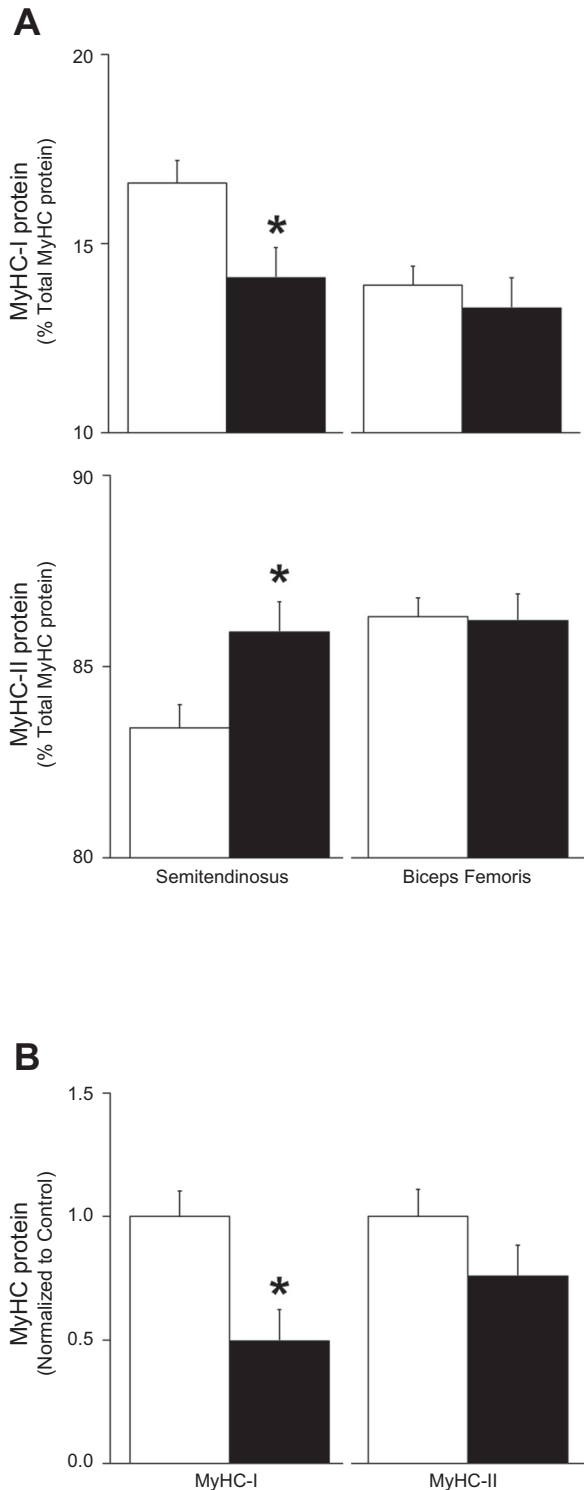


Fig. 4. Myosin heavy chain protein content. Control, open bars; IUGR, black bars. *A*: electrophoretic mobility was used to separate MyHC-I and MyHC-II fractions of total protein isolated from control and IUGR semitendinosus and biceps femoris samples. The percentage of total MyHC protein (means  $\pm$  SE) for MyHC-I and MyHC-II protein content are presented. \*Differences ( $P < 0.05$ ) between control and IUGR groups within each muscle. *B*: semitendinosus MyHC-I and MyHC-II protein content was measured by immunoblot and normalized to  $\beta$ -tubulin content and expressed as the relative density compared with controls (means  $\pm$  SE). \*Differences ( $P < 0.05$ ) between control and IUGR groups.

natal adrenal gland (2). Catecholamines have been shown to affect fetal muscle growth and development (6), and we have demonstrated chronic, progressively worsening hypercatecholaminemia over the third trimester in this model previously (22, 48, 53). In rodents and lambs,  $\beta$ -adrenergic agonists have been shown to reduce the ratio of Type I to Type II fibers (9, 37, 57, 91), presumably due to the differences in adrenergic receptor profiles between the two fiber types (reviewed in Ref. 75). In rat muscle, for example,  $\beta$ -adrenergic receptor densities in Type I fibers are twofold to threefold greater than in Type II

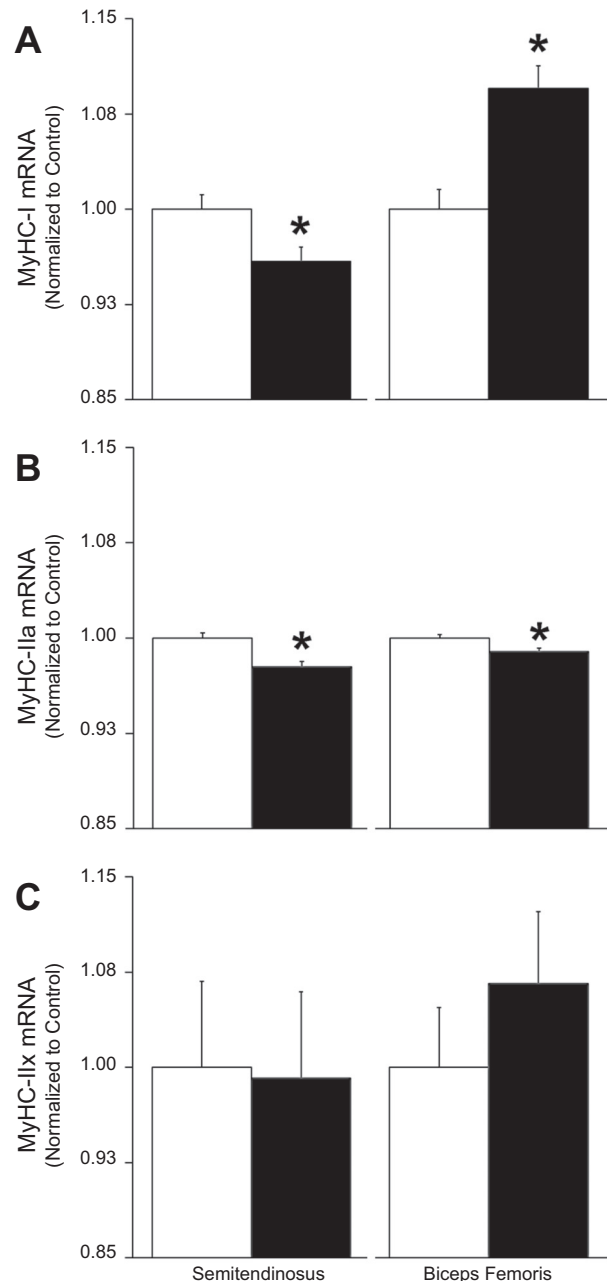


Fig. 5. Myosin heavy chain gene expression. Control, open bars; IUGR, black bars. *A*: MyHC-I; *B*: MyHC-IIa; *C*: MyHC-IIx mRNA concentrations were measured in control and IUGR semitendinosus and biceps femoris samples, normalized to s15 mRNA concentrations and are expressed as amount relative to controls (means  $\pm$  SE). \*Differences ( $P < 0.05$ ) between control and IUGR groups within each muscle.

fibers. Not surprisingly, fiber oxidative capacity closely correlates with adrenergic receptor numbers as well (58, 73, 74). Chronic administration of  $\beta$ -adrenergic agonists to rats substantially downregulated receptor content in the Type I-dominant soleus muscle but did not have the same effect in the Type II-dominant extensor digitorum longus muscle (73, 74). In the present study, higher plasma norepinephrine concentrations were highly correlated with reductions in the proportion of Type I fibers and in the collective proportion of Types I and IIa, and thus it is presumable that chronic stimulation by the high catecholamine levels in our IUGR fetuses reduced the presence of these highly oxidative fibers. Alternatively, high catecholamines or other factors may have delayed the normal perinatal increase of Type I fibers that occurs in most muscles (19, 56). In swine, for example, Type I fibers from naturally growth-restricted (“runt”) piglets showed signs of immature formation at birth that was not present in normal-sized littermates and that disappeared within a few weeks of birth (1). However, maternal nutrient-restriction models of IUGR in sheep show decreased Type I fibers in offspring at 6 mo of age, which indicates a more permanent outcome rather than a transient delay (20).

Reduced ratios of Type I and IIa fibers in IUGR fetuses could have major implications on glucose homeostasis. Skeletal muscle accounts for ~80% of the body’s insulin-stimulated glucose utilization (27), and insulin sensitivity is three- to fourfold higher in Type I fibers and twofold higher in Type IIa fibers than in Type IIx fibers (34, 38, 55). In adults, muscle-specific insulin sensitivity is positively correlated to the percentage of Type I fibers and negatively correlated to the percentage of Type IIx fibers (49), which is likely due to the greater content of insulin receptor, Glut4, and other insulin signaling proteins in Type I fibers (4, 15, 45). Reduced Type I/IIa-to-Type IIx fibers ratios are common in adults suffering from obesity, Type 2 diabetes, and metabolic syndrome (4, 77) and have been linked to IUGR-induced low birth weight in humans and animals (8, 40, 92). Thus it is reasonable to conclude that the differences in fiber-type composition observed in the muscles of our IUGR fetuses are part of an adaptive response that predisposes them to metabolic complications later in life.

Insulin stimulates hypertrophic growth of fibers during late gestation and after birth (reviewed in Ref. 14), and we previously found that adaptive programming in IUGR fetal muscle leads to smaller fibers but not lower fiber density near term (86). However, our previous study did not distinguish between individual fiber types. In our present study, we show that Type I and Type II fibers are uniformly smaller (~32–37%) in both semitendinosus and biceps femoris muscles. It is doubtful that catecholamines were directly responsible for reduced muscle mass in our IUGR fetuses, as  $\beta$ -adrenergic agonists are in fact commonly used to increase lean mass in food animals (9, 10). Rather, it is more likely that rate of muscle growth is decreased by the chronically low insulin concentrations that resulted from the combination of high catecholamines and low glucose concentrations. Indeed, Bassett and Hanson (6, 7) showed that a week-long infusion of catecholamines restricted muscle growth in fetal sheep, but that a simultaneous insulin infusion rescued it. It should be noted that IGF-1 and other important muscle growth factors were not measured in this study but were previously shown to be reduced in IUGR fetal sheep (17, 41,

79, 83). Equivalent reduction in size of the various types of fibers despite their natural differences in insulin and adrenergic sensitivities supports our previous findings that IUGR muscle mass is reduced primarily by decreased myoblast proliferation rates (86).

### Perspectives and Significance

Our findings in near-term IUGR fetal sheep reveal two key adaptive changes in skeletal muscle that may help explain greater propensity for insulin resistance in adulthood. First, we found that the proportions of fibers with highly oxidative phenotypes were reduced in two different hindlimb muscles, but proportions of the more glycolytic fiber types were normal, which would imply lower capacity for insulin-stimulated glucose utilization by these muscles. We speculate that this change results from the greater sensitivity of oxidative fiber types to the physiological conditions induced by placental insufficiency, especially elevated catecholamines. Second, we found that IUGR fibers were uniformly decreased in size regardless of fiber type, which explains greater loss of lean mass and more pronounced asymmetric growth patterns. The fiber type-independent reduction in size also appears to support our previous findings which indicate that poor muscle growth in IUGR fetuses is primarily due to impaired myoblast function. The difference in fiber-type composition and reduction in muscle mass observed in our IUGR fetuses have also been observed in IUGR-born adults with metabolic disorders and could represent mechanistic links for the fetal origins of metabolic dysfunction that increase the risk for obesity and Type 2 diabetes.

### ACKNOWLEDGMENTS

The authors are solely responsible for the content, which does not necessarily represent the official views of the National Institutes of Health or United State Department of Agriculture. The MyHC antibodies were obtained from the Developmental Studies Hybridoma Bank developed under the auspices of the NICHD and maintained by The University of Iowa, Department of Biology, Iowa City, IA.

### GRANTS

This work was supported by Award R01 DK084842 (to S. W. Limesand) from the National Institute of Diabetes and Digestive and Kidney Diseases and by Award 2012-67012-19855 (to D. T. Yates) from the National Institute of Food and Agriculture, USDA. L. E. Camacho was supported by T32 HL7249 (J. Burt) and by Award 2016-67012-24672 (to L. Camacho) from the National Institute of Food and Agriculture, USDA.

### DISCLOSURES

No conflicts of interest, financial or otherwise, are declared by the author(s).

### AUTHOR CONTRIBUTIONS

D.T.Y., L.E.C., and S.W.L. conception and design of research; D.T.Y., C.N.C., K.A.B., H.E.R., A.R.M., M.J.A., L.E.C., and S.W.L. performed experiments; D.T.Y., C.N.C., K.A.B., H.E.R., A.R.M., M.J.A., L.E.C., and S.W.L. analyzed data; D.T.Y., K.A.B., and S.W.L. interpreted results of experiments; D.T.Y. prepared figures; D.T.Y. drafted manuscript; D.T.Y., C.N.C., L.E.C., and S.W.L. edited and revised manuscript; D.T.Y., C.N.C., K.A.B., H.E.R., A.R.M., M.J.A., L.E.C., and S.W.L. approved final version of manuscript.

### REFERENCES

1. **Aberle ED.** Myofiber differentiation in skeletal muscles of newborn runt and normal weight pigs. *J Anim Sci* 59: 1651–1656, 1984.

2. Adams MB, Phillips ID, Simonetta G, McMillen IC. Differential effects of increasing gestational age and placental restriction on tyrosine hydroxylase, phenylethanolamine N-methyltransferase, and proenkephalin A mRNA levels in the fetal sheep adrenal. *J Neurochem* 71: 394–401, 1998.
3. Aihie Sayer A, Syddall HE, Dennison EM, Gilbody HJ, Duggleby SL, Cooper C, Barker DJ, Phillips DI. Birth weight, weight at 1 y of age, and body composition in older men: findings from the Hertfordshire Cohort Study. *Am J Clin Nutr* 80: 199–203, 2004.
4. Albers PH, Pedersen AJ, Birk JB, Kristensen DE, Vind BF, Baba O, Nohr J, Hojlund K, Wojtaszewski JF. Human muscle fiber type-specific insulin signaling: impact of obesity and type 2 diabetes. *Diabetes* 64: 485–497, 2015.
5. Barker DJ, Hales CN, Fall CH, Osmond C, Phipps K, Clark PM. Type 2 (non-insulin-dependent) diabetes mellitus, hypertension and hyperlipidaemia (syndrome X): relation to reduced fetal growth. *Diabetologia* 36: 62–67, 1993.
6. Bassett JM, Hanson C. Catecholamines inhibit growth in fetal sheep in the absence of hypoxemia. *Am J Physiol Regul Integr Comp Physiol* 274: R1536–R1545, 1998.
7. Bassett JM, Hanson C. Prevention of hypoinsulinemia modifies catecholamine effects in fetal sheep. *Am J Physiol Regul Integr Comp Physiol* 278: R1171–R1181, 2000.
8. Beauchamp B, Ghosh S, Dysart MW, Kanaan GN, Chu A, Blais A, Rajamanickam K, Tsai EC, Patti ME, Harper ME. Low birth weight is associated with adiposity, impaired skeletal muscle energetics and weight loss resistance in mice. *Int J Obes (Lond)* 39: 702–711, 2015.
9. Beermann DH, Butler WR, Hogue DE, Fishell VK, Dalrymple RH, Ricks CA, Scanes CG. Cimaterol-induced muscle hypertrophy and altered endocrine status in lambs. *J Anim Sci* 65: 1514–1524, 1987.
10. Bell AW, Bauman DE, Beermann DH, Harrell RJ. Nutrition, development and efficacy of growth modifiers in livestock species. *J Nutr* 128: 360s–363s, 1998.
11. Bell AW, Wilkening RB, Meschia G. Some aspects of placental function in chronically heat-stressed ewes. *J Dev Physiol* 9: 17–29, 1987.
12. Beltrand J, Verkauskiene R, Nicolescu R, Sibony O, Gaucherand P, Chevenne D, Claris O, Levy-Marchal C. Adaptive changes in neonatal hormonal and metabolic profiles induced by fetal growth restriction. *J Clin Endocrinol Metab* 93: 4027–4032, 2008.
13. Bloemberg D, Quadrilatero J. Rapid determination of myosin heavy chain expression in rat, mouse, and human skeletal muscle using multi-color immunofluorescence analysis. *PLoS One* 7: e35273, 2012.
14. Brown LD. Endocrine regulation of fetal skeletal muscle growth: impact on future metabolic health. *J Endocrinol* 221: R13–R29, 2014.
15. Castorena CM, Mackrell JG, Bogan JS, Kanzaki M, Cartee GD. Clustering of GLUT4, TUG, and RUVBL2 protein levels correlate with myosin heavy chain isoform pattern in skeletal muscles, but AS160 and TBC1D1 levels do not. *J Appl Physiol* 111: 1106–1117, 2011.
16. Chen X, Fahy AL, Green AS, Anderson MJ, Rhoads RP, Limesand SW.  $\beta$ -Adrenergic receptor desensitization in perirenal adipose tissue in fetuses and lambs with placental insufficiency-induced intrauterine growth restriction. *J Physiol* 588: 3539–3549, 2010.
17. Chen X, Rozance PJ, Hay WW, Limesand SW. Insulin-like growth factor and fibroblast growth factor expression profiles in growth-restricted fetal sheep pancreas. *Exp Biol Med (Maywood)* 237: 524–529, 2012.
18. Cole L, Anderson M, Antin P, Limesand S. One process for pancreatic  $\beta$ -cell coalescence into islets involves an epithelial-mesenchymal transition. *J Endocrinol* 203: 19–31, 2009.
19. d'Albis A, Couteaux R, Janmot C, Roulet A. Specific programs of myosin expression in the postnatal development of rat muscles. *Eur J Biochem* 183: 583–590, 1989.
20. Daniel ZC, Brameld JM, Craigon J, Scollan ND, Buttery PJ. Effect of maternal dietary restriction during pregnancy on lamb carcass characteristics and muscle fiber composition. *J Anim Sci* 85: 1565–1576, 2007.
21. Danielson L, McMillen IC, Dyer JL, Morrison JL. Restriction of placental growth results in greater hypotensive response to alpha-adrenergic blockade in fetal sheep during late gestation. *J Physiol* 563: 611–620, 2005.
22. Davis MA, Macko AR, Steyn LV, Anderson MJ, Limesand SW. Fetal adrenal demedullation lowers circulating norepinephrine and attenuates growth restriction but not reduction of endocrine cell mass in an ovine model of intrauterine growth restriction. *Nutrients* 7: 500–516, 2015.
23. De Blasio MJ, Gatford KL, McMillen IC, Robinson JS, Owens JA. Placental restriction of fetal growth increases insulin action, growth, and adiposity in the young lamb. *Endocrinology* 148: 1350–1358, 2007.
24. de Boo HA, Eremia SC, Bloomfield FH, Oliver MH, Harding JE. Treatment of intrauterine growth restriction with maternal growth hormone supplementation in sheep. *Am J Obstet Gynecol* 199: 559 e551–e559, 2008.
25. de Boo HA, van Zijl PL, Smith DE, Kulik W, Lafeber HN, Harding JE. Arginine and mixed amino acids increase protein accretion in the growth-restricted and normal ovine fetus by different mechanisms. *Pediatr Res* 58: 270–277, 2005.
26. de Vrijer B, Davidsen ML, Wilkening RB, Anthony RV, Regnault TR. Altered placental and fetal expression of IGFs and IGF-binding proteins associated with intrauterine growth restriction in fetal sheep during early and mid-pregnancy. *Pediatr Res* 60: 507–512, 2006.
27. DeFronzo RA, Jacot E, Jequier E, Maeder E, Wahren J, Felber JP. The effect of insulin on the disposal of intravenous glucose. Results from indirect calorimetry and hepatic and femoral venous catheterization. *Diabetes* 30: 1000–1007, 1981.
28. Desai M, Gayle D, Babu J, Ross MG. Programmed obesity in intrauterine growth-restricted newborns: modulation by newborn nutrition. *Am J Physiol Regul Integr Comp Physiol* 288: R91–R96, 2005.
29. Deveaux V, Picard B, Bouley J, Cassar-Malek I. Location of myostatin expression during bovine myogenesis in vivo and in vitro. *Reprod Nutr Dev* 43: 527–542, 2003.
30. Economides DL, Proudler A, Nicolaides KH. Plasma insulin in appropriate- and small-for-gestational-age fetuses. *Am J Obstet Gynecol* 160: 1091–1094, 1989.
31. Flanagan DE, Moore VM, Godsland IF, Cockington RA, Robinson JS, Phillips DI. Fetal growth and the physiological control of glucose tolerance in adults: a minimal model analysis. *Am J Physiol Endocrinol Metab* 278: E700–E706, 2000.
32. Galan HL, Hussey MJ, Barbera A, Ferrazzi E, Chung M, Hobbins JC, Battaglia FC. Relationship of fetal growth to duration of heat stress in an ovine model of placental insufficiency. *Am J Obstet Gynecol* 180: 1278–1282, 1999.
33. Gale CR, Martyn CN, Kellingray S, Eastell R, Cooper C. Intrauterine programming of adult body composition. *J Clin Endocrinol Metab* 86: 267–272, 2001.
34. Goodyear LJ, Hirshman MF, Smith RJ, Horton ES. Glucose transporter number, activity, and isoform content in plasma membranes of red and white skeletal muscle. *Am J Physiol Endocrinol Metab* 261: E556–E561, 1991.
35. Granlund A, Jensen-Waern M, Essen-Gustavsson B. The influence of the PRKAG3 mutation on glycogen, enzyme activities and fibre types in different skeletal muscles of exercise trained pigs. *Acta Vet Scand* 53: 20, 2011.
36. Greenough A, Nicolaides KH, Lagercrantz H. Human fetal sympathoadrenal responsiveness. *Early Hum Dev* 23: 9–13, 1990.
37. Hayes A, Williams DA. Long-term clenbuterol administration alters the isometric contractile properties of skeletal muscle from normal and dystrophin-deficient mdx mice. *Clin Exp Pharmacol Physiol* 21: 757–765, 1994.
38. Henriksen EJ, Bourey RE, Rodnick KJ, Koranyi L, Permutt MA, Holloszy JO. Glucose transporter protein content and glucose transport capacity in rat skeletal muscles. *Am J Physiol Endocrinol Metab* 259: E593–E598, 1990.
39. Jensen CB, Storgaard H, Dela F, Holst JJ, Madsbad S, Vaag AA. Early differential defects of insulin secretion and action in 19-year-old caucasian men who had low birth weight. *Diabetes* 51: 1271–1280, 2002.
40. Jensen CB, Storgaard H, Madsbad S, Richter EA, Vaag AA. Altered skeletal muscle fiber composition and size precede whole-body insulin resistance in young men with low birth weight. *J Clin Endocrinol Metab* 92: 1530–1534, 2007.
41. Jensen EC, Harding JE, Bauer MK, Gluckman PD. Metabolic effects of IGF-I in the growth retarded fetal sheep. *J Endocrinol* 161: 485–494, 1999.
42. Kellis E, Galanis N, Natsis K, Kapetanios G. Muscle architecture variations along the human semitendinosus and biceps femoris (long head) length. *J Electromyogr Kinesiol* 20: 1237–1243, 2010.
43. Kensara OA, Wootton SA, Phillips DI, Patel M, Jackson AA, Elia M, Grp HS. Fetal programming of body composition: relation between birth weight and body composition measured with dual-energy X-ray absorptiometry and anthropometric methods in older Englishmen. *Am J Clin Nutr* 82: 980–987, 2005.
44. Kirchofer KS, Calkins CB, Gwartney BL. Fiber-type composition of muscles of the beef chuck and round. *J Anim Sci* 80: 2872–2878, 2002.

45. Kong X, Manchester J, Salmons S, Lawrence JC Jr. Glucose transporters in single skeletal muscle fibers. Relationship to hexokinase and regulation by contractile activity. *J Biol Chem* 269: 12963–12967, 1994.
46. Lang U, Baker RS, Khoury J, Clark KE. Effects of chronic reduction in uterine blood flow on fetal and placental growth in the sheep. *Am J Physiol Regul Integr Comp Physiol* 279: R53–R59, 2000.
47. Larciprete G, Valensise H, Di Pierro G, Vasapollo B, Casalino B, Arduini D, Jarvis S, Cirese E. Intrauterine growth restriction and fetal body composition. *Ultrasound Obstet Gynecol* 26: 258–262, 2005.
48. Leos RA, Anderson MJ, Chen X, Pugmire J, Anderson KA, Limesand SW. Chronic exposure to elevated norepinephrine suppresses insulin secretion in fetal sheep with placental insufficiency and intrauterine growth restriction. *Am J Physiol Endocrinol Metab* 298: E770–E778, 2010.
49. Lillioja S, Young AA, Culter CL, Ivy JL, Abbott WG, Zawadzki JK, Yki-Jarvinen H, Christin L, Secomb TW, Bogardus C. Skeletal muscle capillary density and fiber type are possible determinants of in vivo insulin resistance in man. *J Clin Invest* 80: 415–424, 1987.
50. Limesand SW, Hay WW Jr. Adaptation of ovine fetal pancreatic insulin secretion to chronic hypoglycaemia and euglycaemic correction. *J Physiol* 547: 95–105, 2003.
51. Limesand SW, Rozance PJ, Macko AR, Anderson MJ, Kelly AC, Hay WW Jr. Reductions in insulin concentrations and beta-cell mass precede growth restriction in sheep fetuses with placental insufficiency. *Am J Physiol Endocrinol Metab* 304: E516–E523, 2013.
52. Limesand SW, Rozance PJ, Smith D, Hay WW Jr. Increased insulin sensitivity and maintenance of glucose utilization rates in fetal sheep with placental insufficiency and intrauterine growth restriction. *Am J Physiol Endocrinol Metab* 293: E1716–E1725, 2007.
53. Macko AR, Yates DT, Chen X, Green AS, Kelly AC, Brown LD, Limesand SW. Elevated plasma norepinephrine inhibits insulin secretion, but adrenergic blockade reveals enhanced  $\beta$ -cell responsiveness in an ovine model of placental insufficiency at 0.7 of gestation. *J Dev Orig Health Disease* 4: 402–410, 2013.
54. Macko AR, Yates DT, Chen X, Shelton LA, Kelly AC, Davis MA, Camacho LE, Anderson MJ, Limesand SW. Adrenal demedullation and oxygen supplementation independently increase glucose-stimulated insulin concentrations in fetal sheep with intrauterine growth restriction. *Endocrinol*: en20151850, 2016.
55. Mackrell JG, Cartee GD. A novel method to measure glucose uptake and myosin heavy chain isoform expression of single fibers from rat skeletal muscle. *Diabetes* 61: 995–1003, 2012.
56. Maier A, McEwan JC, Dodds KG, Fischman DA, Fitzsimons RB, Harris AJ. Myosin heavy chain composition of single fibres and their origins and distribution in developing fascicles of sheep tibialis cranialis muscles. *J Musc Res Cell Mobil* 13: 551–572, 1992.
57. Maltin CA, Delday MI, Reeds PJ. The effect of a growth promoting drug, clenbuterol, on fibre frequency and area in hind limb muscles from young male rats. *Biosci Rep* 6: 293–299, 1986.
58. Martin W, Murphree S, Saffitz J. Beta-adrenergic receptor distribution among muscle fiber types and resistance arterioles of white, red, and intermediate skeletal muscle. *Circ Res* 64: 1096–1105, 1989.
59. Mericq V, Ong KK, Bazaes R, Pena V, Avila A, Salazar T, Soto N, Iniguez G, Dunger DB. Longitudinal changes in insulin sensitivity and secretion from birth to age three years in small- and appropriate-for-gestational-age children. *Diabetologia* 48: 2609–2614, 2005.
60. Muhlhauser BS, Duffield JA, Ozanne SE, Pilgrim C, Turner N, Morrison JL, McMillen IC. The transition from fetal growth restriction to accelerated postnatal growth: a potential role for insulin signalling in skeletal muscle. *J Physiol* 587: 4199–4211, 2009.
61. Newsome CA, Shiell AW, Fall CH, Phillips DI, Shier R, Law CM. Is birth weight related to later glucose and insulin metabolism?—A systematic review. *Diabet Med* 20: 339–348, 2003.
62. Ong KK, Ahmed M, Emmett PM, Preece MA, Dunger DB. Association between postnatal catch-up growth and obesity in childhood: prospective cohort study. *BMJ* 320: 967–971, 2000.
63. Ozanne S, Jensen C, Tingey K, Storgaard H, Madsbad S, Vaag A. Low birthweight is associated with specific changes in muscle insulin-signalling protein expression. *Diabetologia* 48: 547–552, 2005.
64. Ozanne SE, Jensen CB, Tingey KJ, Storgaard H, Madsbad S, Vaag AA. Low birthweight is associated with specific changes in muscle insulin-signalling protein expression. *Diabetologia* 48: 547–552, 2005.
65. Padoan A, Rigano S, Ferrazzi E, Beaty BL, Battaglia FC, Galan HL. Differences in fat and lean mass proportions in normal and growth-restricted fetuses. *Am J Obstet Gynecol* 191: 1459–1464, 2004.
66. Picard B, Barboiron C, Chadeyron D, Jurie C. Protocol for high-resolution electrophoresis separation of myosin heavy chain isoforms in bovine skeletal muscle. *Electrophoresis* 32: 1804–1806, 2011.
67. Rab M, Mader N, Kamolz LP, Hausner T, Gruber H, Girsch W. Basic anatomical investigation of semitendinosus and the long head of biceps femoris muscle for their possible use in electrically stimulated neosphincter formation. *Surg Radiol Anat* 19: 287–291, 1997.
68. Ravelli AC, van der Meulen JH, Michels RP, Osmond C, Barker DJ, Hales CN, Bleker OP. Glucose tolerance in adults after prenatal exposure to famine. *Lancet* 351: 173–177, 1998.
69. Regnault TR, de Vrijer B, Galan HL, Davidsen ML, Tremblay KA, Battaglia FC, Wilkening RB, Anthony RV. The relationship between transplacental O<sub>2</sub> diffusion and placental expression of PlGF, VEGF and their receptors in a placental insufficiency model of fetal growth restriction. *J Physiol* 550: 641–656, 2003.
70. Regnault TR, de Vrijer B, Galan HL, Wilkening RB, Battaglia FC, Meschia G. Umbilical uptakes and transplacental concentration ratios of amino acids in severe fetal growth restriction. *Pediatr Res* 73: 602–611, 2013.
71. Regnault TR, Galan HL, Parker TA, Anthony RV. Placental development in normal and compromised pregnancies. *Placenta* 23, Suppl A: S119–S129, 2002.
72. Regnault TR, Orbus RJ, de Vrijer B, Davidsen ML, Galan HL, Wilkening RB, Anthony RV. Placental Expression of VEGF, PlGF and their Receptors in a Model of Placental Insufficiency-Intrauterine Growth Restriction (PI-IUGR). *Placenta* 23: 132–144, 2002.
73. Ryall JG, Gregorevic P, Plant DR, Silence MN, Lynch GS.  $\beta_2$ -Agonist fenoterol has greater effects on contractile function of rat skeletal muscles than clenbuterol. *Am J Physiol Regul Integr Comp Physiol* 283: R1386–R1394, 2002.
74. Ryall JG, Plant DR, Gregorevic P, Silence MN, Lynch GS. Beta 2-agonist administration reverses muscle wasting and improves muscle function in aged rats. *J Physiol* 555: 175–188, 2004.
75. Sato S, Shirato K, Tachiyashiki K, Imaizumi K. Muscle plasticity and beta(2)-adrenergic receptors: adaptive responses of beta(2)-adrenergic receptor expression to muscle hypertrophy and atrophy. *J Biomed Biotechnol* 2011: 729598, 2011.
76. Setia S, Sridhar MG, Bhat V, Chaturvedula L, Vinayagamoorti R, John M. Insulin sensitivity and insulin secretion at birth in intrauterine growth retarded infants. *Pathology* 38: 236–238, 2006.
77. Stuart CA, McCurry MP, Marino A, South MA, Howell ME, Layne AS, Ramsey MW, Stone MH. Slow-twitch fiber proportion in skeletal muscle correlates with insulin responsiveness. *J Clin Endocrinol Metab* 98: 2027–2036, 2013.
78. Talmadge RJ, Roy RR. Electrophoretic separation of rat skeletal muscle myosin heavy-chain isoforms. *J Appl Physiol* 75: 2337–2340, 1993.
79. Thorn SR, Regnault TR, Brown LD, Rozance PJ, Keng J, Roper M, Wilkening RB, Hay WW Jr, Friedman JE. Intrauterine growth restriction increases fetal hepatic gluconeogenic capacity and reduces messenger ribonucleic acid translation initiation and nutrient sensing in fetal liver and skeletal muscle. *Endocrinology* 150: 3021–3030, 2009.
80. Thureen PJ, Tremblay KA, Meschia G, Makowski EL, Wilkening RB. Placental glucose transport in heat-induced fetal growth retardation. *Am J Physiol Regul Integr Comp Physiol* 263: R578–R585, 1992.
81. Vickers MH, Breier BH, Cutfield WS, Hofman PL, Gluckman PD. Fetal origins of hyperphagia, obesity, and hypertension and postnatal amplification by hypercaloric nutrition. *Am J Physiol Endocrinol Metab* 279: E83–E87, 2000.
82. Vielwerth SE, Jensen RB, Larsen T, Holst KK, Molgaard C, Greisen G, Vaag A. The effect of birthweight upon insulin resistance and associated cardiovascular risk factors in adolescence is not explained by fetal growth velocity in the third trimester as measured by repeated ultrasound fetometry. *Diabetologia* 51: 1483–1492, 2008.
83. Wali JA, de Boo HA, Derraik JG, Phua HH, Oliver MH, Bloomfield FH, Harding JE. Weekly intra-amniotic IGF-1 treatment increases growth of growth-restricted ovine fetuses and up-regulates placental amino acid transporters. *PLoS One* 7: e37899, 2012.
84. Wallace JM, Milne JS, Aitken RP, Hay WW. Sensitivity to metabolic signals in late-gestation growth-restricted fetuses from rapidly growing adolescent sheep. *Am J Physiol Endocrinol Metab* 293: E1233–E1241, 2007.
85. Woodley SJ, Mercer SR. Hamstring muscles: architecture and innervation. *Cells Tissues Organs* 179: 125–141, 2005.

86. **Yates DT, Clarke DS, Macko AR, Anderson MJ, Shelton LA, Nearing M, Allen RE, Rhoads RP, Limesand SW.** Myoblasts from intrauterine growth-restricted sheep fetuses exhibit intrinsic deficiencies in proliferation that contribute to smaller semitendinosus myofibres. *J Physiol* 592: 3113–3125, 2014.
87. **Yates DT, Green AS, Limesand SW.** Catecholamines mediate multiple fetal adaptations during placental insufficiency that contribute to intrauterine growth restriction: Lessons from hyperthermic sheep. *J Pregnancy*. doi:10.1155/2011/740408, 2011.
88. **Yates DT, Macko AR, Chen X, Green AS, Kelly AC, Anderson MJ, Fowden AL, Limesand SW.** Hypoxaemia-induced catecholamine secretion from adrenal chromaffin cells inhibits glucose-stimulated hyperinsulinaemia in fetal sheep. *J Physiol* 590: 5439–5447, 2012.
89. **Yates DT, Macko AR, Nearing M, Chen X, Rhoads RP, Limesand SW.** Developmental programming in response to intrauterine growth restriction impairs myoblast function and skeletal muscle metabolism. *J Pregnancy* 2012: 631038, 2012.
90. **Yliharsila H, Kajantie E, Osmond C, Forsen T, Barker DJP, Eriksson JG.** Birth size, adult body composition and muscle strength in later life. *Int J Obes* 31: 1392–1399, 2007.
91. **Zeman RJ, Ludemann R, Easton TG, Etlinger JD.** Slow to fast alterations in skeletal muscle fibers caused by clenbuterol, a  $\beta_2$ -receptor agonist. *Am J Physiol Endocrinol Metab* 254: E726–E732, 1988.
92. **Zhu MJ, Ford SP, Means WJ, Hess BW, Nathanielsz PW, Du M.** Maternal nutrient restriction affects properties of skeletal muscle in offspring. *J Physiol* 575: 241–250, 2006.

